

Collisional enhancement of Rydberg lifetimes observed in vibrational wave packet experiments

Marc J. J. Vrakking,^{a)} Ingo Fischer,^{b)} D. M. Villeneuve, and Albert Stolow
Ultrafast Phenomena Group, Steacie Institute for Molecular Sciences, National Research Council of Canada, Ottawa, Ontario, Canada K1A 0R6

(Received 1 May 1995; accepted 14 June 1995)

Evidence for lifetime enhancement of Rydberg states by interactions with surrounding ions is obtained from femtosecond pump-probe experiments on the vibrational wave packet dynamics of the $I_2(B)$ -state, in which either detection of I_2^+ ions or zero-kinetic energy (ZEKE) electrons was used. The use of the ZEKE technique leads to the appearance of new frequency components in the Fourier transform power spectra of pump-probe time delay scans, as well as the observation of enhanced peak-to-valley ratios in these scans. These observed frequency components do not correspond to any energy level spacings in the molecule; they correspond to a sum of two energy level spacings, suggesting a nonlinear detection mechanism in the ZEKE technique (i.e., interaction with ions). Additional evidence for our interpretation is presented through experiments in which additional ions were formed through nonresonant multiphoton ionization of I_2 with a picosecond 266 nm laser, as well as experiments in which both the decay time of the ZEKE signal and the appearance of the pump-probe time delay scans as a function of the pulsed field time delay were studied. Theoretical wave packet calculations which support the conclusions are presented. © 1995 American Institute of Physics.

I. INTRODUCTION

In recent years, there has been considerable interest in the lifetimes of high principal quantum number Rydberg states. This interest was caused primarily by numerous observations in zero-kinetic-energy (ZEKE) photoelectron spectroscopy experiments in which the lifetimes of high- n Rydberg states were found to be considerably longer than what would be expected based upon extrapolation of known lifetimes from low- n members of the relevant Rydberg series.^{1,2} Considerations of both intramolecular, intermolecular, and external field effects on high- n Rydberg lifetimes have been discussed by several authors.³⁻³⁶

Two models have been suggested to account for the observed lifetimes of the high- n Rydberg states. First, Levine and co-workers have suggested that the lifetimes of the high- n Rydberg states are determined by energy exchange between the Rydberg electron and the rotational degrees of freedom of the ionic core.^{5-10,13} This energy exchange may lead both to quenching of the Rydberg states and the long term stability of the Rydberg states. The latter case occurs in particular when the energy exchange is associated with an increase in the angular momentum l of the Rydberg electron,¹³ and a breakdown of the Born-Oppenheimer approximation ensues. The dynamics of the Rydberg electron is envisioned in terms of "up" and "down" processes, describing the transfer of the Rydberg electron to higher- n and lower- n Rydberg states.⁶ This model has been discussed recently by other authors.^{4,22}

As an alternate model, Chupka suggested^{3,4} that the life-

times of the high- n Rydberg states might be enhanced by processes which alter the angular momentum quantum numbers l and m of the Rydberg electron, notably l -mixing in small dc electric fields (which are inevitably present in ZEKE experiments) and l, m -mixing due to interactions of the Rydberg electron with surrounding ions. In a dc electric field the orbital angular momentum l is no longer a good quantum number since the spherical symmetry is broken by the presence of the field. The eigenstates are Stark states, characterized by the quantum numbers n , k (the parabolic quantum number) and m .³⁷⁻³⁹ When the Stark states are expressed in terms of the field-free eigenstates characterized by n , l , and m , one finds that many different values of l contribute to a given Stark state. The decay rate of a Rydberg state is determined by close-range interactions of the Rydberg electron with the ionic core. Therefore the decay rate depends strongly on the orbital angular momentum l and, for molecules, its projection onto the molecular frame. Typically, decay rates are large for low- l orbitals and significantly smaller for nonpenetrating orbitals with $l > 3$. It follows that when an electric field mixes angular momentum states, the lifetimes of the Stark states can be longer than the lifetimes of the field-free low- l states, since the contribution of these low- l angular momentum states to the wave function is reduced. This is indeed what was observed in recently reported experiments on the NO molecule,^{25,26} where dc electric field induced lifetime enhancements of nearly two orders of magnitude were observed when the rapidly predissociating p -orbital, which dominates in the absorption spectrum, becomes mixed with the stable high- l states. It was argued that under typical ZEKE conditions the stray dc electric fields are such that the Rydberg states which are detected by pulsed field ionization are l -mixed Stark states.

If a Rydberg atom or molecule is excited in the presence of a nearby ion, the electrostatic interaction of the Rydberg

^{a)}Present address: Laser Centre Free University Amsterdam, Physical & Theoretical Chemistry, De Boelelaan 1083, 1081 HV, Amsterdam, The Netherlands.

^{b)}Present address: Laboratorium für Organische Chemie der ETH Zürich, Universitätsstr. 16, CH-8092, Zürich.

electron with the ion also causes l -mixing, similar to the case of an externally applied dc electric field. If the Rydberg atom or molecule experiences an electrostatic interaction from multiple surrounding charges, or the combined interaction from a nearby ion and a small stray dc electric field,²⁰ as discussed above, then both the spherical and the cylindrical symmetry of the electric field are broken. In this case neither the orbital angular momentum l (or its body-fixed projection), nor the magnetic quantum number m is a good quantum number.^{37,40–43} Compared with the case of pure l -mixing considered in the previous paragraph, the lifetime of Rydberg states is further enhanced due to the $(2l+1)$ -fold m -degeneracy of the l -states, favoring high- l components in the electronic wave functions over low- l components. Evidence for an ion-Rydberg mechanism was obtained in recently reported experiments on the lifetimes of autoionizing Rydberg states of the Xe atom.²⁷ It was observed that all the observable pulsed field ionization signals showed a near-quadratic dependence on the Xe pressure, i.e., the detection probability of the Xe Rydberg states was near-linear in the density of surrounding Xe⁺ ions. The experiments on Xe showed clear evidence that an interplay can exist between dc electric field effects and “collisional” effects in ZEKE. While all the autoionizing Xe Rydberg states required (l,m) -mixing by surrounding ions in order to be detected, the process was aided considerably when l -mixing was introduced at the outset using a small dc electric field.

The influence of Rydberg–ion interactions has been inferred by a number of other authors.^{15,19,24,36} In measurements of lifetimes of predissociating Rydberg states of NO (Ref. 15) by Pratt and of autoionizing Rydberg states of Ar (Ref. 19) by Merkt, it was concluded that the observed lifetime enhancements with respect to extrapolated field-free lifetimes could only be obtained by invoking a mechanism which involved both l - and m -mixing. In recent experiments on Rydberg states of the HD molecule, Zare and co-workers observed that the magnitude of pulsed field ionization signals was increased by the addition of extra ions.³⁶ Zhang *et al.* concluded that the lifetimes of high- n Rydberg states of styrene, phenol, phenanthrene, and iron were reduced by collisional ionization through Rydberg–Rydberg or Rydberg–ion interactions.²⁴ Bahatt *et al.* looked for collisional effects in studies of lifetimes of Rydberg states of phenanthrene, but no effect was observed.⁵ Schlag and co-workers have recently investigated the role of Rydberg–ion interactions on lifetimes of Rydberg states of normal and perdeuterated benzene.³⁵ They looked for changes in the ZEKE spectra when a controlled number of ions was introduced in the interaction region, without seeing any effect. In comparing their results to the aforementioned Xe results,²⁷ they suggested that there may be a fundamental difference between small atomic and large I₂ molecular systems, with respect to the production of Rydberg-ZEKE states.

Schlag and co-workers have also recently discussed the possible role of electron-transfer processes in ZEKE experiments.^{11,14} They observed the formation of long-lived Rydberg states formed by charge transfer between the high- n Rydberg state and a nearby ionic core. They concluded that at typical laser intensities the electron transfer represents a

minor channel, although they expected that this will change at high laser intensities.¹¹ While the occurrence of such processes certainly is possible, we do not believe that charge transfer plays a significant role in our I₂ experiments, to be discussed below. The onset for charge transfer between an $n=100$ Rydberg state and a neighboring ion takes place at an internuclear distance of approximately $6n^2=3.2 \mu\text{m}$.^{14,33} The onset for l,m -mixing Rydberg–ion interactions for an $n=100$ Rydberg is at an internuclear distance of approximately $50 \mu\text{m}$.^{20,27} Therefore it is anticipated that l,m -mixing will become important at significantly lower densities than charge transfer. Typical ion densities in the I₂ experiments to be reported below were 10^6 – 10^7 cm^{-3} , where charge transfer ought to be a minor channel.

In this paper, results are presented for a femtosecond pump–probe experiment which provides considerable further evidence for the lifetime enhancement of Rydberg states due to interactions with the surrounding ions. The vibrational wave packet dynamics of the I₂ molecule in the B -state was studied^{44,45} by detecting, as a function of the time delay between the femtosecond preparation and femtosecond probing of the B -state, either prompt I₂⁺ ions or electrons formed by pulsed field ionization of high- n Rydberg states (i.e., ZEKE), both produced via (1+2) multiphoton excitation. The experiments using the ZEKE technique provide evidence for lifetime enhancement of the I₂ Rydberg states due to the presence of surrounding I₂⁺ and I⁺ ions. This lifetime enhancement leads to the observation of an increase in the peak-to-valley ratio in the pump–probe time delay scans. This is the case because, as with the Rydberg states themselves, the density of the I₂⁺ and I⁺ ions which enhance the Rydberg lifetimes, also depends on the time delay between the pump and probe lasers. It will be demonstrated that the dependence of the ion and Rydberg densities on the pump–probe time delay is described by a small set of frequencies which relate to energy differences between vibrational eigenstates in the I₂(B) molecule and that the lifetime enhancement of the Rydberg states introduces new frequency components in the time dependence of the ZEKE signal which *do not* correspond to any energy difference between eigenstates of the molecule. The observation of these new frequency components, which arise as cross-terms between the frequencies describing the production of Rydberg states and ions, respectively, is a general indicator of a nonlinear detection mechanism. Additional evidence for the Rydberg–ion interactions, illustrating our ability to amplify the pump–probe ZEKE signal by the introduction of ions in the interaction region, and a simple theoretical model are presented to support these conclusions.

Briefly returning to the issue of charge transfer, we note that in these experiments approximately equal amounts of I⁺ and I₂⁺ ions were produced. Therefore charge transfer should lead to the formation of significant numbers of atomic Rydberg states, with anticipated lifetimes of many microseconds. These lifetimes are incommensurate with the lifetimes of the Rydberg states which were experimentally observed. In our experiments no ZEKE signals could be observed beyond pulsed field delay times of approximately 2–3 μs , in agreement with recent nanosecond ZEKE experiments on I₂ by

Donovan and co-workers.⁴⁶ We also note that this lifetime (2–3 μs) is much shorter than the measured “lifetime” of ions in the viewing region of our spectrometer—which was significantly greater than 10 μs —and therefore our pulsed-field signals cannot be due to kinetic electrons trapped by plasma effects. Therefore, in the remainder of this paper, we will discuss the influence of the surrounding I^+ and I_2^+ ions on the lifetime of the I_2 Rydberg states in terms of l, m -mixing.

II. EXPERIMENT

A comprehensive description of the experimental apparatus is presented elsewhere^{45,47} and therefore we will only discuss the most important features here. Briefly, in a molecular beam ZEKE photoelectron spectrometer, the $\text{I}_2(B)$ state is populated using a 90 fs pump pulse tuned near 580 nm. The pump laser is based on three-stage dye amplification of a selected part of a white light continuum, generated when part of an amplified Tsunami Ti:Sapphire laser is focused into a quartz flat. A similar dye amplifier is used to generate the probe pulse; a 130 fs pulse is generated near 690 nm and is frequency-doubled in a 0.1 mm BBO crystal. The 345 nm pulse produced is used to excite I_2 to the ionization continuum and to the high- n Rydberg states, through a two-photon absorption from the B -state. The observations consist of monitoring either the I_2^+ signal or the ZEKE signal as a function of the time delay between the 580 nm pump and 345 nm probe lasers, as discussed below. It is important to note that the ion detection scheme uses a dc extraction field (i.e., all the ions are prompt), while the ZEKE measurement is sensitive only to the delayed pulsed field ionization of Rydberg states.

In order to vary the time delay between the pump and probe lasers, the 580 nm laser is retroreflected using a computer controlled motorized delay stage, prior to entering the molecular beam chamber. The 580 nm and 345 nm pulses are combined on a dichroic beamsplitter, transmitting the visible beam and reflecting the ultraviolet beam, and are focused into the molecular beam apparatus using a 400 mm lens positioned such that the focus of the 345 nm pulse is close to the molecular beam axis and the spot size of the 580 nm pulse is reduced to about 1 mm. Typical energies of the pump and probe lasers were about 10 $\mu\text{J}/\text{pulse}$ each. The pump and probe lasers have parallel polarizations. At the lens, the diameter of the 345 nm beam is approximately 2 mm, and thus the spot size of the 345 nm laser at the molecular beam is expected to be about 100 μm . The width of the molecular beam in the interaction region is about 3 mm, and therefore the volume of the interaction region is approximately $3 \times 10^{-5} \text{ cm}^3$. In typical ion detection experiments, the number of I_2^+ and I^+ ions produced was estimated to be 10^2 , in approximately equal amounts. Therefore, assuming a homogeneous ion distribution within the detection volume, ion densities on the order of $3 \times 10^6 \text{ cm}^{-3}$ were produced. Under these conditions the ZEKE signal was less than 10 counts per laser shot. As will be discussed in detail below, the ZEKE signal could be enhanced substantially by creating additional ions. Therefore, typical ZEKE experiments were carried out at ion densities on the order of 10^7 cm^{-3} , yielding

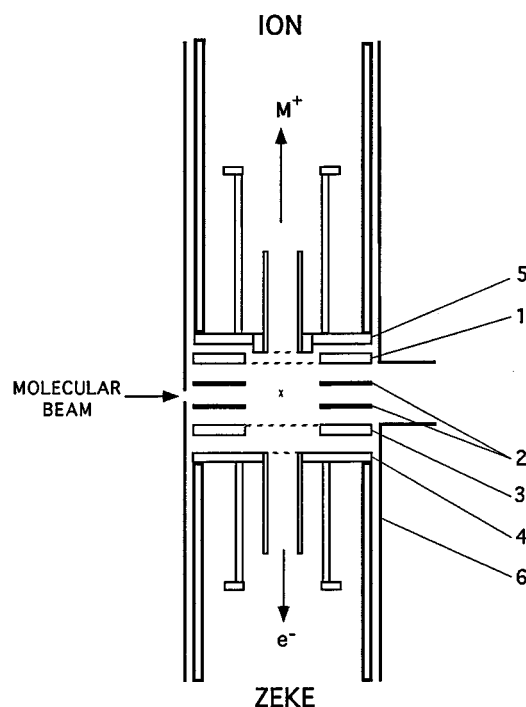


FIG. 1. Schematic of the interaction region of the experiment. The two extraction grids (1) and (3) are separated by 2 cm, and form the entrance to two time-of-flight spectrometers [labeled (4) and (5)], one for the detection of ions and one for the detection of electrons. In addition to the meshes, two guard rings, labeled (2), improve the homogeneity of the extraction fields. The electron spectrometer is surrounded by a thick-walled μ -metal tube (6).

a ZEKE signal of 10 – 10^2 electrons per laser shot. This corresponds to a density of detectable Rydberg states of 3×10^5 – $3 \times 10^6 \text{ cm}^{-3}$.

The interaction region of the experiment is shown in Fig. 1. The crossing point of the laser beams and the pulsed molecular beam is located between two extraction meshes [labeled (1) and (3)], which are separated by 2 cm. These form the entrance to two time-of-flight spectrometers [labeled (4) and (5)], one for the detection of ions and one for the detection of electrons [two guard rings, labelled (2), serve to improve the homogeneity of the extraction fields]. When detecting I_2^+ , a +500 V dc voltage is applied to electrode (3), while electrode (1) is held at ground (i.e., the extraction field is 250 V/cm). When detecting ZEKE electrons, all extraction electrodes are at ground potential when the laser beams pass through the apparatus, and a small voltage pulse (typically -8 V , 5 ns rise time, 1 μs duration, i.e., the extraction field is 4 V/cm) is applied to electrode (1) after a delay of 100 ns–1 μs . This voltage pulse ionizes the surviving high- n Rydberg molecules and accelerates the ZEKE electrons towards the microchannel plate detector. The electron spectrometer sits inside a thick-walled μ -metal tube [labeled (6)], reducing the earth’s magnetic field by measured factors of 500 in the axial direction and 1000 in the radial direction. It is well known that stray electric fields can play a considerable role in ZEKE experiments.^{3,10,15,19,25,26} The absolute magnitude of the stray electric field could not be determined in the current experiment, however, the fact that ZEKE sig-

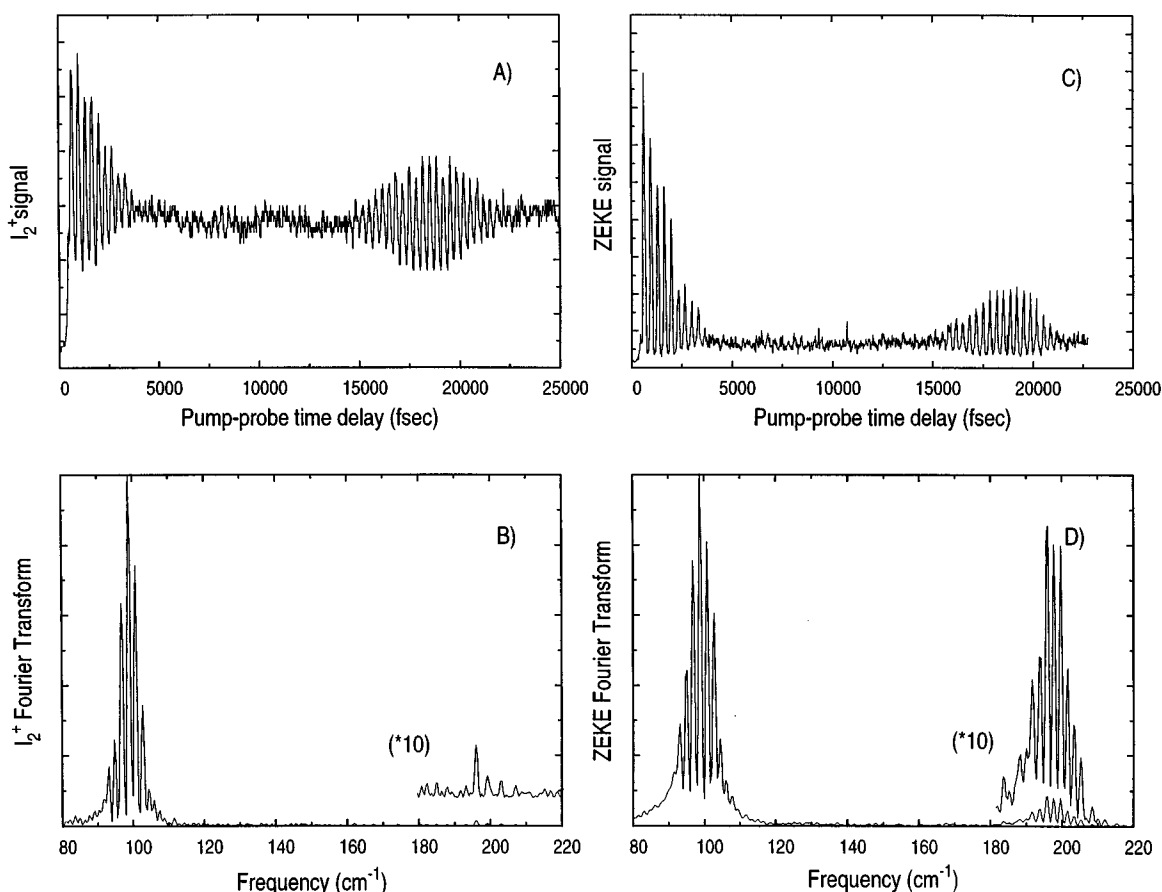


FIG. 2. Comparison of the experimental $I_2(B)$ pump-probe time delay scans and corresponding Fourier transforms when using I_2^+ detection and ZEKE detection. The scan given in frame (a) shows the I_2^+ signal as a function of the delay between the 580 nm pump laser and the 345 nm probe laser. The Fourier transform power spectrum (FT) of this scan is shown in frame (b). The scan given in frame (c) shows the ZEKE signal as a function of the delay between the two lasers. The ZEKE signal was collected by applying a 4 V/cm electric field after a 1 μ s delay. The FT of the ZEKE spectrum is shown in frame (d), and shows a substantial 2ω contribution, as discussed in the text.

nals could be recorded efficiently with extraction pulses as small as 1 V suggests that the stray electric fields were well below 500 mV/cm. Since all electrodes consist of chemically cleaned molybdenum and the base pressure of the vacuum chamber is 2×10^{-10} Torr, we expect the actual stray fields to be on the order of 10–20 mV/cm.

III. RESULTS AND DISCUSSION

A. Wave packet dynamics of I_2

There have been several pump-probe experiments on vibrational wave packet dynamics of diatomic molecules using ultrafast lasers.^{48,49} Therefore we will refrain from a detailed discussion, introducing only the features essential to this work.

We consider first the preparation of a coherent wave packet in the $I_2(B)$ state. In our experiments, I_2 is excited using a femtosecond laser at 580 nm. This laser prepares a coherent superposition of vibrational eigenstates in the B -state centered around $v \approx 15$, in other words, a vibrational wave packet. The different eigenstates each evolve in time according to their individual quantum phase factors $\exp[-i2\pi c E_v(B)t]$, where $E_v(B)$ is the vibrational term value (in cm^{-1}), and as a result the wave packet starts to

move. Specifically, the wave packet moves back and forth between the inner and outer turning point of the B -state potential well with a period given by the *average* vibrational level spacing of the prepared vibrational levels. For $v \approx 15$, the period of the wave packet oscillation is approximately 340 fs. Due to anharmonicity in the interatomic potential, the vibrational level spacing changes as a function of vibrational level. Consequently, a phase mismatch accumulates between the phase factors of the individual vibrational levels, and the wave packet dephases after a number of oscillations. However, since the evolution of the individual eigenstates is coherent, at a later time the wave packet rephases. For $v \approx 15$, this rephasing occurs after a time delay of about 18 ps.

Next we consider the probing of the wave packet. The signal which is measured upon excitation with the 345 nm laser depends on the overlap of the wave packet with the energetically accessible ionic states. As the wave packet moves back and forth in the B -state potential well, it alternately passes through regions of more and less favorable overlap. As a result, the pump-probe time delay scans display modulations which reflect the motion of the wave packet in the B -state potential well. An example is given in Fig. 2(a), showing the I_2^+ signal which is detected as a func-

tion of the delay between the pump and probe pulses. The measurement reflects all the features of the wave packet evolution in the B -state which were described above. Initially 340 fs modulations are seen, reflecting the oscillation of the wave packet in the B -state potential well. The modulations disappear when the wave packet dephases, until, at a time delay of about 18 ps, the wave packet rephases. For a detailed account on the simulation of $I_2(B)$ pump-probe time delay scans including rotational effects as well as a discussion of the information which can be obtained from such an analysis, the reader is referred to the article of Gruebele and Zewail.⁵⁰

The pump-probe experiment can also be described using an eigenstate picture. Since the $I_2(B)$ state vibrational levels are populated coherently, the transition amplitudes must be added up and squared afterwards, in order to get the transition probability. In this picture, the modulations in the time delay scan arise from interferences between transitions from different vibrational levels in the B -state to the same ionic/Rydberg final state. Pairwise interferences between different vibrational levels in the B -state result in contributions to the time dependence of the signal at frequencies corresponding to the energy difference between the two states in question. A FT of the experimental results in Fig. 2(a) is shown in Fig. 2(b) and reveals the frequency content of the pump-probe time delay scan. It is observed that the I_2^+ scan is almost exclusively the result of a series of nearest-neighbor coherences between levels $[v]$ and $[v+1]$ (subsequently referred to as ω components). While nearest-neighbor coherences often dominate in wave packet dynamics experiments, it should be noted that this is by no means required. In a full discussion of our I_2 experiments,⁴⁵ results will be presented where, after changing the wavelength of the probe laser, substantial next-nearest-neighbor coherences (i.e., coherences between $[v]$ and $[v+2]$, subsequently referred to as 2ω components) are observed. These are associated with changes in the optimum point of overlap (the Condon point) between the B -state and the ionic/Rydberg states.

B. Experimental differences in time delay scans using ion and ZEKE detection

In Fig. 2(c), a pump-probe time delay scan, obtained when using the ZEKE technique, is presented. The signals were collected with a 1 μ s delay between the probe laser excitation and the pulsed field ionization and extraction. As in the ion detection results of Fig. 2(a), the ZEKE detection experiment shows the 340 fs oscillation of the wave packet in the B -state potential well, as well as its dephasing and subsequent rephasing after about 18 ps. This is to be expected because, with the ZEKE detection, we are observing the *same* B -state wave packet with a *different* detection technique. A striking difference between the ion and ZEKE results shown in Figs. 2(a) and 2(c) is in the modulation depth, defined as

$$\text{Modulation depth} = (I_{\text{peak}} - I_{\text{valley}}) / (I_{\text{peak}} + I_{\text{valley}}) \times 100. \quad (1)$$

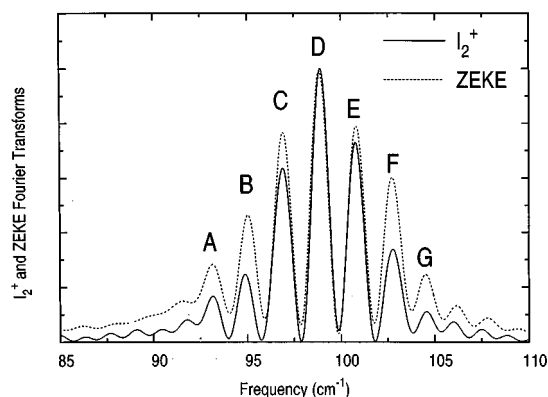


FIG. 3. Comparison of the experimentally observed nearest-neighbor coherences (called ω components) at frequencies near 100 cm^{-1} , when recording pump-probe time delay scans using I_2^+ detection and ZEKE detection. The assignments are given in Table I.

In the I_2^+ scan of Fig. 2(a), at short time delays, the modulation depth is 54%, and after the wave packet dephases, the signal drops to about one-half of the peak signal. By contrast, in the ZEKE scan [Fig. 2(c)] at short time delays, the modulation depth is 91% and after the wave packet dephases, the signal drops to no more than 10% of the peak signal.

The difference between the I_2^+ scan and the ZEKE scan is also reflected in the FTs. The FT of the ZEKE scan, Fig. 1(d), shows a significant 2ω contribution which is nearly absent in the I_2^+ results. The FTs of the I_2^+ and ZEKE scans are compared in detail in Figs. 3 and 4. Assignments of peaks A–G in Fig. 3 and peaks H–O in Fig. 4 are given in Table I and will be discussed below. As seen in Fig. 3, the nearest-neighbor coherences appear with comparable strength in the I_2^+ scan and the ZEKE scan. In Fig. 4, however, the situation is very different for the 2ω components. The 2ω components are significantly stronger in the ZEKE scan, and furthermore, there are some 2ω components which appear in the FT of the ZEKE scan, and *not* in that of the I_2^+ scan (those marked by a * in Fig. 4). In the I_2^+ scan no more than three small peaks,

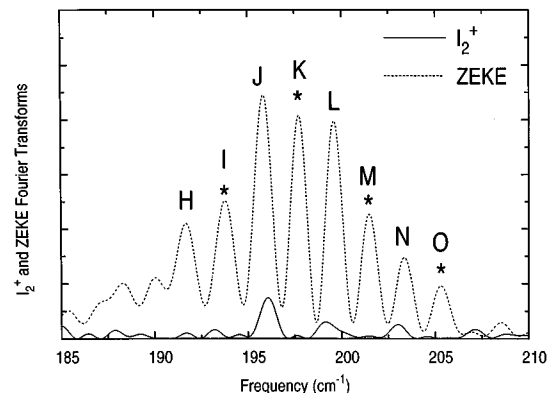


FIG. 4. Comparison of the experimentally observed 2ω frequency components when recording pump-probe time delay scans using I_2^+ detection and ZEKE detection. The peaks labeled by a * do not correspond to energy level spacings in the isolated molecule and arise from interactions between the Rydberg molecules and surrounding ions, which enhance the Rydberg lifetimes (see text for details). Assignments are given in Table I.

TABLE I. Observed frequency components in the Fourier transform power spectra of the I_2^+ and ZEKE time delay scans, with assignments in terms of $I_2(B)$ vibrational level spacings.

ω component	I_2^+ scan (cm^{-1})	ZEKE scan (cm^{-1})	Nearest-neighbor coherence
A	93.16	93.15	$\Delta E_1(18)$
B	94.88	95.02	$\Delta E_1(17)$
C	96.90	96.91	$\Delta E_1(16)$
D	98.89	98.85	$\Delta E_1(15)$
E	100.76	100.79	$\Delta E_1(14)$
F	102.74	102.71	$\Delta E_1(13)$
G	104.56	104.50	$\Delta E_1(12)$

2ω component	I_2^+ scan (cm^{-1})	ZEKE scan (cm^{-1})	Next-nearest neighbor coherence	Combination of nearest-neighbor coherences
H	...	191.67	$\Delta E_2(16)$	$\Delta E_1(15) + \Delta E_1(18)$
I	...	193.77		$2\Delta E_1(16), \Delta E_1(15) + \Delta E_1(17)$
J	196.07	195.82	$\Delta E_2(15)$	$\Delta E_1(14) + \Delta E_1(17)$
K	...	197.71		$2\Delta E_1(15), \Delta E_1(14) + \Delta E_1(16)$
L	199.17	199.60	$\Delta E_2(14)$	$\Delta E_1(13) + \Delta E_1(16)$
M	...	201.47		$2\Delta E_1(14), \Delta E_1(13) + \Delta E_1(15)$
N	203.00	203.36	$\Delta E_2(13)$	$\Delta E_1(12) + \Delta E_1(15)$
O	...	205.31		$2\Delta E_1(13), \Delta E_1(12) + \Delta E_1(14)$

separated by nearly 4 cm^{-1} , can confidently be assigned. In the ZEKE scan eight peaks are seen, separated by nearly 2 cm^{-1} . In what follows, we will argue that the peaks which are weakly observed in the FT of the I_2^+ scan are the ones which are expected from next-nearest-neighbor coherences (i.e., coherences between vibrational levels $[v\rangle$ and $[v+2\rangle$). The narrowly spaced 2ω components in the ZEKE scan, however, point to a nonlinear aspect of the ZEKE detection scheme.

We emphasize that differences between the I_2^+ and the ZEKE scans are due to a difference in the detection scheme employed and not an aspect of the pump-probe experiment itself. In femtosecond pump-probe experiments laser intensities are typically in a regime of 10^{10} – 10^{12} W/cm^2 , where nonlinear interactions of the lasers with the molecules need to be considered. Phenomena such as population-cycling (i.e., Rabi oscillation) and alteration of the potential curves of the molecule in the laser field can occur. In the current experiments, however, since the conditions for the I_2^+ scan and the ZEKE scan were similar, any laser intensity effects must appear in both the I_2^+ and the ZEKE results. We specifically checked that the appearance of the I_2^+ pump-probe time delay scans was independent of the pump and probe laser intensities used in these experiments. In our experiments, it is only afterwards, when we choose to detect either I_2^+ ions or ZEKE electrons, that a difference is observed. Thus this difference reflects a difference in the detection mechanism and is not an aspect of the pump-probe experiment itself.

C. Analysis of observed ω and 2ω components using I_2^+ detection and ZEKE detection

The vibrational energy levels of a diatomic molecule are given to second order by

$$E(v) = \omega_e(v + 1/2) - \omega_e x_e(v + 1/2)^2. \quad (2)$$

Consequently, as illustrated in Fig. 5, the energy difference between levels $[v\rangle$ and $[v+1\rangle$ (i.e., nearest neighbors) is given by

$$\Delta E_1(v) = E(v+1) - E(v) = \omega_e - \omega_e x_e(2v+2) \quad (3)$$

and the energy difference between $[v\rangle$ and $[v+2\rangle$ (i.e., next-nearest neighbors) is given by

$$\Delta E_2(v) = E(v+2) - E(v) = 2\omega_e - \omega_e x_e(4v+6). \quad (4)$$

The relation between $\Delta E_1(v)$ and $\Delta E_2(v)$ is given by

$$\Delta E_2(v) = \Delta E_1(v) + \Delta E_1(v+1). \quad (5)$$

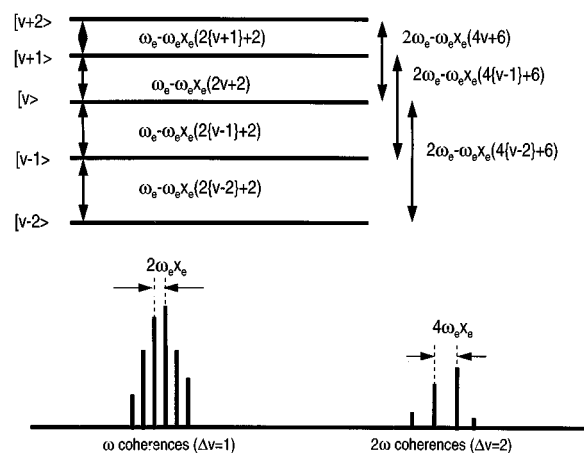


FIG. 5. Schematic vibrational energy level diagram of a diatomic molecule, illustrating the possible energy differences between vibrational states that can give rise to ω and 2ω frequency components in the FT power spectra of the pump-probe time delay scans.

Vibrational assignments for the nearest-neighbor coherences follow from the detailed analysis by Gruebele and Zewail⁵⁰ and are given in Table I. Gruebele and Zewail fit Dunham expansion parameters to a large number of observed vibrational energy differences and determined that $Y_{20} = \omega_e x_e = 0.825(35) \text{ cm}^{-1}$. The average spacing between the peaks in Fig. 3 is 1.87 cm^{-1} , which, according to Eq. (3) represents the *average* energy difference between $\Delta E_1(v) - \Delta E_1(v+1) = 2\omega_e x_e$ in the spectral region of interest. Therefore, if we use the expansion truncated to second order given in Eq. (2), we need to take $\omega_e x_e \approx 1.87/2 = 0.935 \text{ cm}^{-1}$. This is in reasonable agreement with the precise value of Gruebele and Zewail, theirs resulting from the use of an expansion of the vibrational term value to sixth order.

The spacing between successive 2ω components is given by the energy difference between $\Delta E_2(v)$ and $\Delta E_2(v+1)$, which according to Eq. (4) is given by $4\omega_e x_e \approx 3.74 \text{ cm}^{-1}$. Indeed, this is the approximate spacing which is observed for the very weak 2ω components in the I_2^+ scan and thus these peaks can readily be assigned in terms of energy differences between vibrational states $[v]$ and $[v+2]$ [see Table I, where assignments are given for peaks J, L, and N in terms of the next-nearest-neighbor energy differences $\Delta E_2(v)$]. By contrast, the average spacing between the significantly stronger 2ω components in the ZEKE scan is only 1.95 cm^{-1} , i.e., approximately one-half of the expected spacing. Consequently, half of the observed 2ω components, namely the ones labeled * in Fig. 4, *cannot* be related to energy differences between pairs of vibrational levels in the *B*-state of I_2 . They cannot, therefore, originate from the *isolated* molecule. For example, with reference to Fig. 5, we would anticipate a 2ω component at successive energies of $2\omega_e - \omega_e x_e(4v+6)$ and $2\omega_e - \omega_e x_e[4(v-1)+6] = 2\omega_e - \omega_e x_e(4v+2)$. We *should not* be able to detect a 2ω component halfway between these two frequencies, at $2\omega_e - \omega_e x_e(4v+4)$; a simple picture interpreting the 2ω components in terms of coherences between vibrational levels $[v]$ and $[v+2]$ cannot explain the data. We can, however, assign all the observed lines, as discussed below.

While the observed 2ω components cannot be related to energy differences in the I_2 molecule, the regularity of the frequencies which appear in the ZEKE scan suggests that the 2ω components are still related to energy differences in the molecule. For example, the large peak labeled K appears at the frequency corresponding to $2\Delta E_1(15)$ and/or $\Delta E(14) + \Delta E_1(16)$. In fact, all of the “forbidden” lines I, K, M, and O can be assigned as the sum of two nearest-neighbor frequencies, as shown in Table I. We suggest that the mechanism which causes the new frequencies consists of a lifetime enhancement of the Rydberg states under the influence of surrounding I^+/I_2^+ ions, as discussed in detail below.

With this mechanism, the observations of an enhanced modulation depth in the ZEKE scans and the appearance of additional 2ω components in the FT of the ZEKE time delay scan can be rationalized in the following way. First, lifetime enhancement of the Rydberg states due to the presence of surrounding ions will have an impact on the modulation depth since not only the concentration of Rydberg molecules

but also the concentration of the surrounding I^+/I_2^+ ions is modulated. When the overlap of the wave packet with the ionic/Rydberg state is favorable, a large number of Rydberg states is produced and these Rydberg states are detected efficiently since, as can be seen from Fig. 2(a), they are embedded in a large number of surrounding I^+/I_2^+ ions. On the other hand, when the overlap of the wave packet with the ionic/Rydberg state is poor, the number of Rydberg states is reduced and furthermore these Rydberg states are not detected as efficiently, since fewer I^+/I_2^+ ions are produced as well. As a result, an increased modulation depth of the ZEKE signal is expected, similar to what is seen in Fig. 2(c). It is possible in principle that an enhanced modulation depth is due to the final state selectivity of the ZEKE technique. That is to say, ZEKE is a differential as opposed to integrated detection technique for femtosecond pump-probe experiments, as discussed in Ref. 44. However, in Sec. III D we present further experimental evidence that the surrounding ions significantly affect the modulation depths.

Let $S_{\text{ION}}(\Delta t)$ be the number of ions produced at pump-probe time delay Δt , as in Fig. 2(a). If we assume that the ion-Rydberg interaction can be characterized by binary interactions, then the probability that a Rydberg molecule will undergo a lifetime enhancement, allowing for detection, is proportional to $S_{\text{ION}}(\Delta t)$. This assumption is supported by the recently reported experiments on lifetime enhancement of autoionizing Xe Rydberg states through ion-Rydberg interactions in which the pulsed field ionization signal was found to be approximately quadratic in the Xe pressure,²⁷ as well as experimental observations to be discussed in Sec. III D. Therefore we assume that the detection probability of the Rydberg molecules has the same modulation as the ion signal in Fig. 2(a). Similar to the ion production, the number of Rydberg molecules produced is proportional to $S_{\text{ION}}(\Delta t)$. The ZEKE signal $S_{\text{ZEKE}}(\Delta t)$ is given as the product of the number of Rydberg molecules produced [$\sim S_{\text{ION}}(\Delta t)$] and the detection probability of the Rydberg molecules [$\sim S_{\text{ION}}(\Delta t)$], hence

$$S_{\text{ZEKE}}(\Delta t) \sim [S_{\text{ION}}(\Delta t)]^2. \quad (6)$$

Modulations in $S_{\text{ION}}(\Delta t)$ will lead to more pronounced modulations in $S_{\text{ZEKE}}(\Delta t)$. We note that in these experiments the I^+ ions were formed through dissociation of I_2^+ , and thus the time dependence of the I^+ concentration closely resembles that of the I_2^+ concentration.

Secondly, lifetime enhancement of the Rydberg states due to the presence of surrounding ions will lead to the introduction of new frequencies in the FT of the ZEKE signal. When the ZEKE spectrum is measured according to Eq. (6), cross-terms arise between the various frequency components in $S_{\text{ION}}(\Delta t)$, and it is possible to form 2ω combinations from the ω components in $S_{\text{ION}}(\Delta t)$. These new 2ω combinations are separated by $2\omega_e x_e$, the frequency difference between the ω components. To illustrate this, consider again the 2ω component at frequency $2\omega_e - \omega_e x_e(4v+4)$. While this frequency does not correspond to an existing difference between the energy of two eigenstates, we *can*, for example, obtain this frequency as the second harmonic of the next-neighbor coherence

$\Delta E_1(v) = \omega_e - \omega_e x_e(2v+2)$, or as the sum-frequency of the two next-neighbor coherences $\Delta E_1(v-1) = \omega_e - \omega_e x_e(2v)$ and $\Delta E_1(v+1) = \omega_e - \omega_e x_e(2v+4)$. Although, with our resolution, we cannot determine uniquely which nearest-neighbor coherences are responsible for the 2ω components observed in the ZEKE scan, the tentative assignments given in Table I illustrate that for all the peaks observed, likely candidates can readily be found. All these assignments correspond to a sum of the frequencies of *two* nearest-neighbor coherences where, in our interpretation, one frequency is due to the pump-probe delay time dependence of the Rydberg population and the other arises from the pump-probe delay time dependence of the concentration of the surrounding I^+/I_2^+ ions. A simple theoretical model illustrating the above conclusions is presented in Sec. III E.

D. Additional experimental evidence for lifetime enhancement through Rydberg-ion interactions.

There are a number of additional experimental observations associated with our ZEKE experiments which support the hypothesis that the difference between the modulation depths in the time delay scans and the frequencies in the FTs of the I_2^+ and ZEKE scans arises from lifetime enhancement of the Rydberg states due to the influence of Rydberg-ion interactions. There are several qualitative observations which led us to investigate the role of Rydberg lifetimes in these experiments. First, it was noticed that the ZEKE signal at 1 μ s extraction delay depended nonlinearly on the pump laser power; when the I_2^+ , I^+ , and ZEKE signals were monitored as a function of the pump laser power, it was observed that the ion signals scaled linearly with laser power, whereas the ZEKE signal scaled at least quadratically with the total number of ions (within the range of laser powers used in our ZEKE experiments). Large ZEKE signals could be observed at lower pump laser powers, provided that the pulsed field time delay was reduced to about 100 ns. When using a 100 ns pulsed field time delay the modulation depth decreased to 80%, as shown in Fig. 6. A decrease in the modulation depth in the ZEKE scan is expected if there is a contribution to the ZEKE signal which does not require a lifetime enhancement. As will be illustrated below, the “half-life” of the high- n I_2 Rydberg states is of the order of 100 ns. In order to record a ZEKE signal at a 1 μ s pulsed field time delay, this lifetime needs to be enhanced. We suggest that this is accomplished by introducing l, m -mixing interactions due to the surrounding I^+/I_2^+ ions. At a pulsed field time delay of 100 ns, a mixture of Rydberg states will be detected which may or may not have undergone a lifetime enhancement and, thus, the 80% modulation depth is intermediate between the 54% modulation depth of the I_2^+ scan and the 91% modulation depth of the ZEKE scan at a 1 μ s pulsed field time delay.

Two further experiments were performed. If the Rydberg states can be stabilized through interactions with surrounding ions, then it should not matter how these ions were originally produced. In order to test this idea, a 400 μ J pulse of frequency-quadrupled light (from a picosecond Nd:YAG laser) was introduced into the interaction region, about 40 ns before the arrival of the femtosecond pulses. This 266 nm, 80 ps pulse nonresonantly ionized I_2 , producing excess ions;

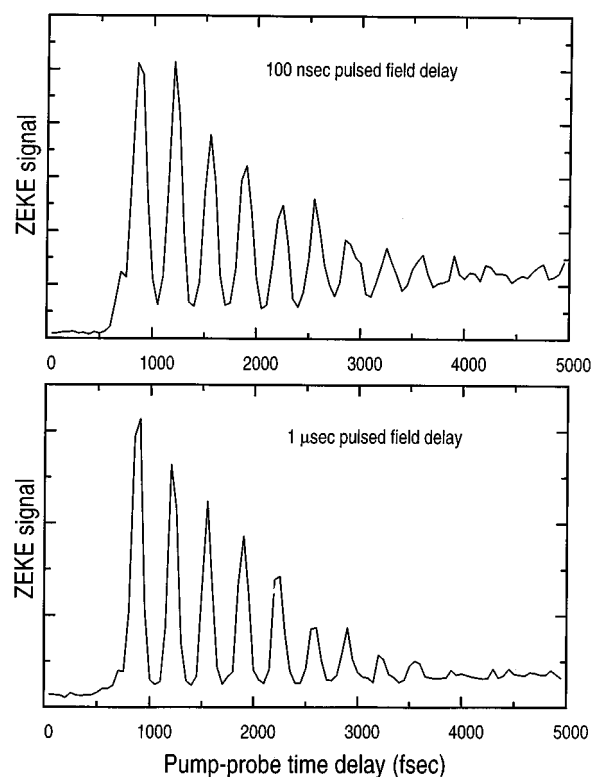


FIG. 6. Comparison between the pump-probe time delay scan recorded using ZEKE detection, when the 4 V/cm ionization field is turned on after (top) 100 ns and (bottom) 1 μ s. The measurement at 1 μ s displays a greater modulation depth, as well as a smaller dc component at longer time delays, when the wave packet has dephased.

namely, a measured tenfold increase over the number of ions produced in the pump-probe experiment itself. This implies an average ion density in the detection volume of up to 3×10^7 cm^{-3} , depending on how well the volume in which the additional ions were produced matched the detection volume of the pump-probe experiment. We note that there was no evidence that this laser produced significant numbers of Rydberg states.

In the first experiment we considered the effect of the 266 nm laser on the magnitude of the ZEKE signal and the modulation depths in the scan. If the presence of excess ions leads to an enhancement of the Rydberg lifetimes, then we expect that the pump-probe ZEKE signal should increase. Furthermore, because the density of the excess ions is independent of the pump-probe time delay, a smaller modulation depth (i.e., closer to the 54% modulation depth of the I_2^+ scan) is expected. Indeed, as shown in Fig. 7, it was experimentally observed that the pump-probe ZEKE signal at 1 μ s increased about sixfold under these conditions (i.e., the 266 nm laser acted as an “amplifier” of the ZEKE signal), and furthermore, in the ZEKE scan the modulation depth decreased to 68%, in agreement with our expectations. We note that the sixfold ZEKE signal enhancement mentioned above was observed under the condition where the results of Figs. 2 and 7(middle) were recorded. As discussed in the Introduction to this paragraph, in order to obtain these results it was necessary to increase the pump laser power beyond the minimum level required in an ion detection experiment. Alterna-

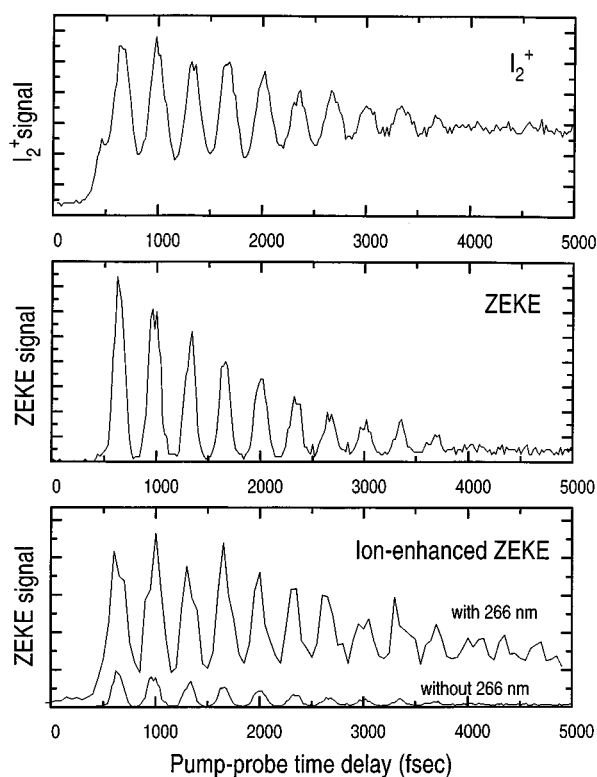


FIG. 7. Comparison of pump-probe time delays using (top) I_2^+ detection; (middle) ZEKE detection at a $1 \mu\text{s}$ time delay for the 4 V/cm ionization field; (bottom) ZEKE detection at a $1 \mu\text{s}$ time delay for the 4 V/cm ionization field when additional ions have been produced with a $400 \mu\text{J}$ 80 ps 266 nm laser pulse. The introduction of the 266 nm laser led to a sixfold enhancement in the ZEKE signal [for comparison, the ZEKE spectrum without the 266 nm laser (middle) is reproduced to scale in (bottom)] as well as a reduction in the modulation depth of the ZEKE signal and an increase in the signal level at long time delays when the wave packet has dephased.

tively, in the presence of the ions produced by the 266 nm laser, it was possible to obtain adequate ZEKE signals at a $1 \mu\text{s}$ time delay at pump laser powers at or below the levels used in the ion detection experiments. In this latter case it was possible to achieve a situation where the actual enhancement of the ZEKE signal through the presence of ions produced by the 266 nm laser was almost two orders of magnitude, since very few ions were produced by the pump and probe lasers.

The lifetimes of the Rydberg states were also explicitly studied by measuring the ZEKE signal as a function of the pulsed field time delay, with and without the additional ions produced by the 266 nm laser. In order to get the clearest assessment of the role of surrounding ions on the lifetime of the Rydberg states, these measurements were performed with the pump laser power reduced to 20% of that used in the measurements discussed above. In this case, the number of ions produced by the pump and probe lasers alone was only 2% of the number of ions produced by the 266 nm laser. The results are shown in Fig. 8. It is observed that without the 266 nm laser, the ZEKE signal drops to nearly zero in about 200–300 ns. By contrast, with the 266 nm laser, the decay of the Rydberg population is significantly slower. At a delay of $1 \mu\text{s}$, where the experiments shown in Fig. 2(bottom) were

performed, the ZEKE signal is still at almost 20% of the zero pulsed field time delay signal level. In fact, pump-probe time delay scans can readily be performed at pulsed field time delays of several microseconds. The observation of enhanced Rydberg lifetimes under the influence of the ions produced by the 266 nm laser (Fig. 8) supports our interpretation of the sixfold signal enhancement observed in Fig. 7 in terms of an ion-induced lifetime enhancement.

We point out that the observed lifetime enhancement in the presence of the 266 nm laser supports the identification of the I_2^+ and I^+ ions as the species which are responsible for the Rydberg lifetime enhancement. In principle, one might anticipate that electrons which are formed along with the I_2^+ and I^+ ions could also be instrumental in changing the angular momentum quantum numbers of the Rydberg electrons. However, electrons formed by the 266 nm laser pulse leave the interaction region during the 40 ns interval between the 266 nm laser pulse and the arrival of the fs pump- and probe-pulses. After the 40 ns interval the only charged species left behind which can influence the I_2 Rydberg molecules are the I_2^+ and I^+ ions produced by the 266 nm laser.

E. Theoretical calculations of I_2^+ and ZEKE spectra

In this section, calculations are presented which support the interpretation of the ZEKE time delay scan and FT in terms of an ion-induced lifetime enhancement. Simple wave packet calculations are presented to describe the I_2^+ signal as a function of the delay between the pump and probe lasers. Using the assumptions (1) that the population of the I_2 Rydberg states follows the production of the I_2^+ ions and (2) that the probability of the detection of the Rydberg states scales linearly with the number of ions produced [Eq. (6)], the FT of the ZEKE signal is presented, and an assessment is made of the presence of 2ω components in this FT.

We stress the fact that assumption (2) is an approximation which is not expected to be valid over a wide range of ion densities. For example, at larger ion densities than the ones quoted in this paper, we do not expect a binary interaction approximation to be valid. Once all the Rydberg states that are excited have undergone a lifetime enhancement, an increase in the ion density will not enhance the signal any further. As another example, as discussed in the Introduction, in the absence of l -mixing by stray dc electric fields, the lifetime enhancement by surrounding ions may involve three-body interactions. Also, as discussed in the introduction, mechanisms have been suggested which do not involve Rydberg-ion interactions.^{5–10,13} A number of ZEKE experiments are known to us in which the authors observed that the detection probability of the Rydberg states *did not* scale linearly with the pressure or the number of ions.^{5,24,35} In our experiments it was observed that the detection probability of the Rydberg states depended on the number of I_2^+ and I^+ ions in a near-linear fashion. The purpose of the current section is mainly to illustrate that our lifetime enhancement model produces the right order of magnitude of 2ω Fourier intensities when using assumption (2).

Initially, an I_2^+ pump-probe time delay scan was calculated by evaluating the time-dependence of the overlap of the B -state wave packet with the lowest vibrational states of the

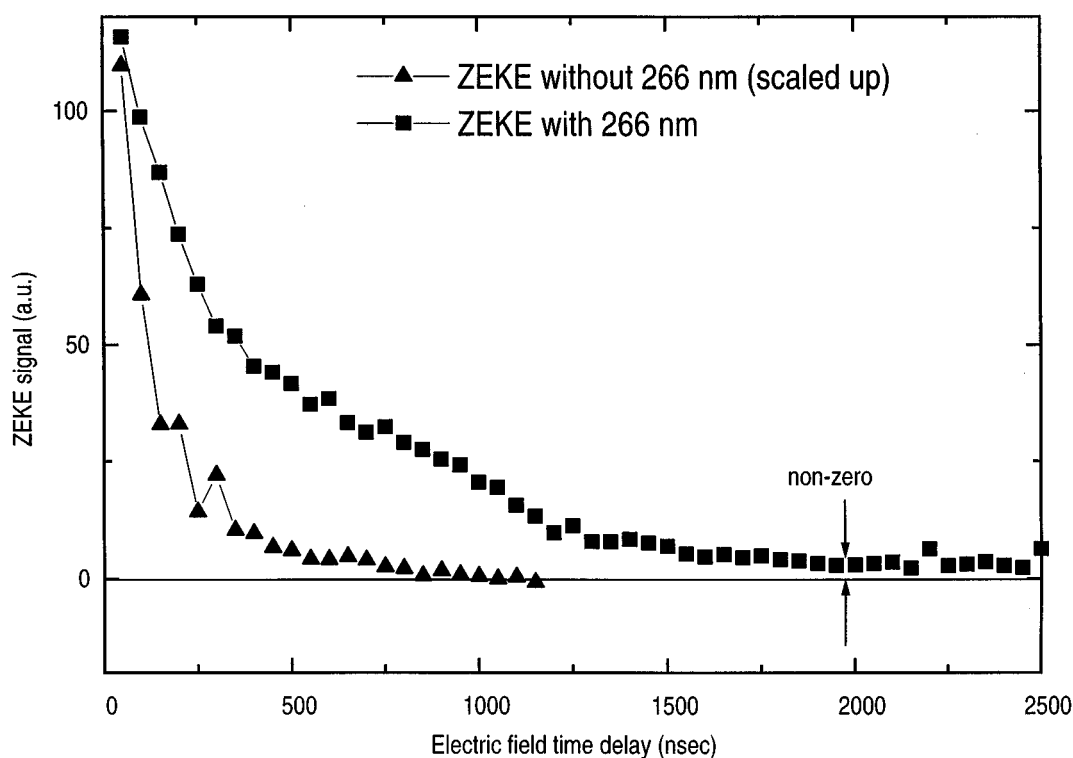


FIG. 8. Comparison of the ZEKE signal as a function of the pulsed field ionization delay time, with and without the presence of 400 μJ of a 80 ps 266 nm laser pulse. The decay curves were recorded at a low pump laser energy, chosen such that without the 266 nm laser no ZEKE signal could be detected at a 1 μs time delay. The signals have been scaled such that the signal levels at the shortest time delay are approximately equal (N.B. at the low pump laser power used in this case, the actual signal with the 266 nm pulse is more than one order of magnitude larger than the signal without the 266 nm).

I_2^+ ion. In this calculation vibrational wave functions in the $\text{I}_2(B)$ -state and in the I_2^+ ground state were computed using the algorithm developed by Cooley,⁵¹ consisting of the application of 6th order Numerov integration in a predictor-corrector method. Morse potentials were used to represent both the $\text{I}_2(B)$ -state and the I_2^+ ground state. In the case of the $\text{I}_2(B)$ -state, we started with the constants given by Herzberg⁵² and adjusted the force constant to obtain agreement with the experimental vibrational level spacings. Morse parameters for the I_2^+ ground state were determined from a fit to recent ZEKE spectra.⁵³ The calculation assumed an instantaneous preparation of the B -state with a 580 nm central wavelength and an 8 nm bandwidth. The probing was also calculated assuming instantaneous excitation with a 345 nm central wavelength and a 5 nm bandwidth. Rotation of the I_2 molecule was neglected in all calculations, justified by the fact that rotations occur on a much longer time scale than vibrations.^{50,54}

A more realistic simulation of the I_2^+ pump-probe time delay scan was obtained when the calculated time delay scan was convoluted with a Gaussian function representing our experimental time-resolution of approximately 150 fs. A FT of the calculated I_2^+ pump-probe time delay scan revealed dominant ω -components as well as smaller 2ω components, similar to the FT of the experimental results [Fig. 2(a)]. The simulated I_2^+ scan was filtered in order to remove the 2ω components altogether. The advantage of this complete removal of the 2ω components is that it facilitates discussion of the appearance of new 2ω components in the ZEKE scan.

If the FT of the I_2^+ scan already contains a 2ω component, then the ZEKE scan will contain a superposition of this 2ω component and the new 2ω components which arise as a result of the lifetime enhancement. In this sense, our experimental observation of an I_2^+ scan with virtually no 2ω component was fortunate, since it presented a situation where the contrast between the 2ω components in the I_2^+ and ZEKE results was very dramatic.

The resulting simulation of the I_2^+ scan after all harmonic components were removed is shown in Fig. 9(a). Comparison of this simulated I_2^+ scan with the experimental I_2^+ scan of Fig. 2(a) shows reasonable agreement. The main difference between the simulated scan and the theoretical scan is the magnitude of the recursion at 18 ps. This difference is largely due to the neglect of rotational effects in the simulation. In addition, the modulation depth in the experimental spectrum is somewhat smaller than in the simulation. This difference is at least partially due to the fact that the experimental I_2^+ may contain background contributions from higher order pump-processes, which do not yield a clear modulation pattern. In fact, when the probe laser was tuned below the ionization potential of I_2 a very small signal without pronounced modulation could be observed.

In Fig. 9(b) the FT of the simulated I_2^+ scan is shown. As a result of the filtering procedure described above, this FT shows exclusively ω components, unlike the FT of the experimental I_2^+ scan, which contains some very small 2ω contributions. However, these small 2ω components do not sig-

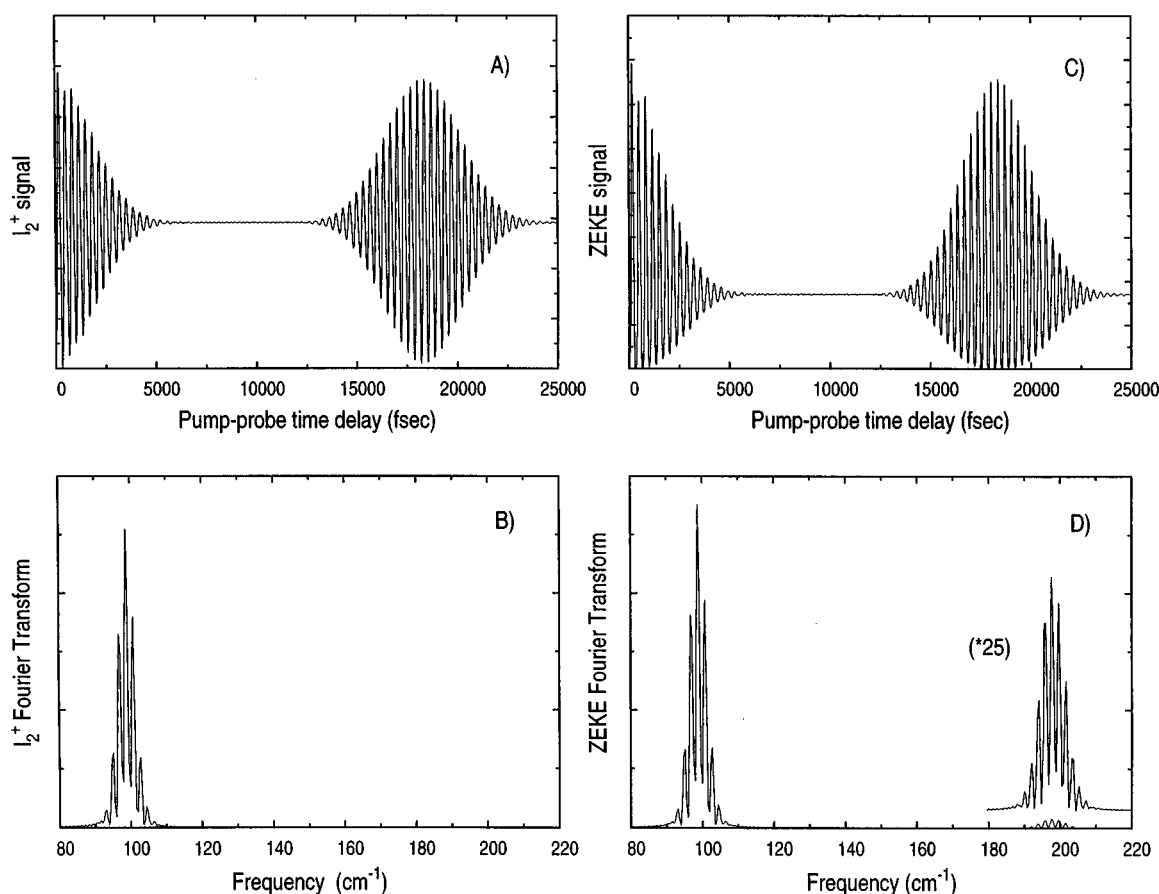


FIG. 9. Comparison of the simulated pump-probe time delay spectra and corresponding FTs when using I_2^+ detection and ZEKE detection. The scan given in frame (a) shows the I_2^+ signal as a function of the delay between the 580 nm pump laser and the 345 nm probe laser. The FT of this scan is shown in frame (b). The scan given in frame (c) shows the ZEKE signal as a function of the delay between the two lasers. The ZEKE scan was calculated as the square of the I_2^+ spectrum according to Eq. (6). The FT of the ZEKE scan is shown in frame (d), and shows a substantial 2ω contribution, with a spacing between the 2ω components which is one-half of that expected for the isolated molecule.

nificantly affect the appearance of the pump-probe time delay scan.

In Fig. 9(c) a ZEKE time delay scan is shown, which was calculated from the simulated I_2^+ scan using Eq. (6), i.e., under the assumption that detection probability of the Rydberg state scales with the number of I^+/I_2^+ ions. In other words, the calculated ZEKE time delay scan is the square of the calculated I_2^+ time delay scan. Due to the ion-induced lifetime enhancement, the ZEKE time delay scan shows a larger modulation depth than the I_2^+ scan, in agreement with our experimental results. The modulation depth is not quite as pronounced as in the experimental ZEKE time delay scan [Fig. 2(c)]. Two possible reasons can be given for this. First of all, the use of the simple model implied by Eq. (6) is an approximation which need not be valid at all ion densities, as discussed above. Furthermore, as discussed above, the experimental I_2^+ scan may contain a small “near-dc” component involving higher-order probe processes, which aid in the lifetime enhancement of the Rydberg states but do not produce Rydberg states.

The FT of the simulated ZEKE scan is shown in Fig. 9(d). In contrast to the FT of the simulated I_2^+ scan [Fig. 9(b)], the FT of the simulated ZEKE scan shows the appearance of 2ω components, which are separated by approxi-

mately 2 cm^{-1} , in agreement with the FT of the experimental ZEKE scan of Fig. 4. Thus the simulations demonstrate that ion-induced lifetime enhancement is a mechanism which can introduce narrowly-spaced 2ω components into the FT, including 2ω components which do not correspond to existing energy level spacings in the molecule. The reasonable agreement between the absolute magnitudes of the 2ω components in the FTs of the experimental and simulated ZEKE scans and the near-absence of 2ω components in the experimental I_2^+ scan lead us to conclude that the 2ω components in the experimental ZEKE FT are almost exclusively due to the lifetime enhancement mechanism discussed in this paper.

IV. CONCLUSION

In this paper we have compared femtosecond pump-probe experiments on the $I_2(B)$ -state employing detection of either I_2^+ or ZEKE electrons produced by REMPI. We have shown that the Rydberg states which are probed in the ZEKE experiments undergo a lifetime enhancement due to interactions with surrounding ions which manifests itself in the time delay scans through the introduction of new frequencies in the Fourier transform power spectrum of the ZEKE scan and the observation of an increased modulation depth. The obser-

vation of narrowly spaced 2ω combination in the experimental ZEKE scan provides perhaps the clearest and most direct indication of the presence of an *intermolecular* aspect to the experiment. Without any prior knowledge about the actual conditions in the experiment, the observation of these 2ω frequency combinations, which do not correspond to any energy difference between molecular eigenstates, provides an indication that the experiment involves a nonlinearity in the detection, leading to a “sum-frequency mixing” of the frequencies which legitimately arise from nearest-neighbor coherences. In our experiments, the observation of an enhanced modulation depth as well as a number of additional experimental observations allowed us to determine that the nonlinear detection is due to a lifetime enhancement of the Rydberg states through interactions with surrounding ions.

Our experiments on lifetime enhancement in Rydberg states of I_2 through Rydberg–ion interactions reach conclusions similar to the experiments on NO by Pratt,¹⁵ the experiments on Ar by Merkt,¹⁹ the experiments on NO and Xe by Vrakking and Lee,^{26,27} and the experiments on HD by Zare and co-workers.³⁶ These observations contrast with the studies by Bahatt *et al.* on phenanthrene,⁵ and those of Alt *et al.* on benzene,³⁵ in which no influence of the presence of ions on Rydberg lifetimes was observed. They also contrast with the studies of Zhang *et al.*, in which the lifetimes of Rydberg states of styrene, phenol, phenanthrene, and iron were reduced by the presence of ions.²⁴ Alt *et al.* have suggested that there may be a fundamental difference between the lifetimes of Rydberg states of small atomic (or molecular) systems and those of large molecular systems.³⁵ In order to determine whether or not this suggestion is correct, there is a clear need for experiments which explicitly investigate the transition in the lifetime dependence on external perturbations, as one goes from the atomic/small molecule limit to the large molecule limit.

Finally, we summarize the evidence for the lifetime enhancement of the I_2 Rydberg states through l,m -mixing caused by surrounding ions. We have presented six different arguments which support this interpretation. In our pump–probe time delay experiments we found (1) an increased modulation depth in the ZEKE scans and (2) the appearance of additional frequencies in the Fourier transform power spectra of the ZEKE scans. (3) We found that the ZEKE signal scaled nonlinearly with the number of I^+/I_2^+ ions produced in the detection volume. (4) The ZEKE signal could be enhanced significantly when additional ions were independently produced with the 4th harmonic of a picosecond Nd:YAG laser and (5) under these conditions, the modulation depth in the ZEKE scan decreased. (6) Furthermore, a measurement of the average lifetime of the Rydberg states showed the presence of a long-lived component with a half-life of several hundred ns, which was absent without the additional ions produced by the Nd:YAG laser.

ACKNOWLEDGMENTS

We thank Professor W. A. Chupka, Professor J. Jortner, and Professor E. W. Schlag for making Refs. 33, 34, and 35 available to us prior to publication and acknowledge Professor R. N. Zare and Dr. M. C. R. Cockett for private commu-

nications. B. Avery, D. Roth, and D. Joines are acknowledged for technical assistance. A. S. acknowledges the Steacie Institute for generous financial support. I. F. acknowledges the Deutsche Forschungsgemeinschaft for a Postdoctoral Fellowship.

- ¹(a) K. Müller-Dethlefs and E. W. Schlag, *Annu. Rev. Phys. Chem.* **42**, 109 (1991); (b) K. Müller-Dethlefs, *J. Chem. Phys.* **95**, 4821 (1991); (c) I. Fischer, R. Lindner, and K. Müller-Dethlefs, *J. Chem. Soc. Faraday Trans.* **90**, 2425 (1994).
- ²G. Reiser, W. Habenicht, K. Müller-Dethlefs, and E. W. Schlag, *Chem. Phys. Lett.* **152**, 119 (1988).
- ³W. A. Chupka, *J. Chem. Phys.* **98**, 4520 (1993).
- ⁴W. A. Chupka, *J. Chem. Phys.* **99**, 5800 (1993).
- ⁵D. Bahatt, U. Even, and R. D. Levine, *J. Chem. Phys.* **98**, 1744 (1993).
- ⁶U. Even, M. Ben-nun, and R. D. Levine, *Chem. Phys. Lett.* **210**, 416 (1993).
- ⁷U. Even, R. D. Levine, and R. Bersohn, *J. Phys. Chem.* **98**, 3472 Z(1994).
- ⁸E. Rabani, L. Ya. Baronov, R. D. Levine, and U. Even, *Chem. Phys. Lett.* **221**, 473 (1994).
- ⁹E. Rabani, R. D. Levine, and U. Even, *J. Phys. Chem.* **98**, 8834 (1994).
- ¹⁰E. Rabani, R. D. Levine, A. Mühlpfordt, and U. Even, *J. Chem. Phys.* **102**, 1619 (1995).
- ¹¹C. Alt, W. G. Scherzer, H. L. Selzle, and E. W. Schlag, *Chem. Phys. Lett.* **224**, 366 (1994).
- ¹²W. G. Scherzer, H. L. Selzle, and E. W. Schlag, *Z. Naturforsch.* **48a**, 1256 (1994).
- ¹³W. G. Scherzer, H. L. Selzle, E. W. Schlag, and R. D. Levine, *Phys. Rev. Lett.* **72**, 1435 (1994).
- ¹⁴C. E. Alt, W. G. Scherzer, H. L. Selzle, E. W. Schlag, L. Ya. Baronov, and R. D. Levine, *J. Phys. Chem.* **99**, 1660 (1995).
- ¹⁵S. T. Pratt, *J. Chem. Phys.* **98**, 9241 (1993).
- ¹⁶S. T. Pratt, *J. Chem. Phys.* **101**, 8302 (1994).
- ¹⁷F. Merkt, H. H. Fielding, and T. P. Softley, *Chem. Phys. Lett.* **202**, 153 (1993).
- ¹⁸F. Merkt and T. P. Softley, *Int. Rev. Phys. Chem.* **12**, 205 (1993).
- ¹⁹F. Merkt, *J. Chem. Phys.* **100**, 2623 (1994).
- ²⁰F. Merkt and R. N. Zare, *J. Chem. Phys.* **101**, 3495 (1994).
- ²¹E. Lee, D. Farrelly, and T. Uzer, *Chem. Phys. Lett.* **231**, 241 (1994).
- ²²J. Jortner and M. Bixon, *J. Chem. Phys.* **102**, 5636 (1995).
- ²³M. Bixon and J. Jortner, *J. Phys. Chem.* **99**, 7466 (1995).
- ²⁴X. Zhang, J. M. Smith, and J. L. Knee, *J. Chem. Phys.* **99**, 3133 (1993).
- ²⁵M. J. J. Vrakking and Y. T. Lee, *Phys. Rev. A* **51**, R894 (1995).
- ²⁶M. J. J. Vrakking and Y. T. Lee, *J. Chem. Phys.* **102**, 8818 (1995).
- ²⁷M. J. J. Vrakking and Y. T. Lee, *J. Chem. Phys.* **102**, 8833 (1995).
- ²⁸J. Berkowitz and B. Ruscic, *J. Chem. Phys.* **93**, 1741 (1990).
- ²⁹G. P. Bryant, Y. Jaing, M. Martin, and E. R. Grant, *J. Phys. Chem.* **96**, 6875 (1992).
- ³⁰G. R. Janik, O. C. Mullins, C. R. Mahon, and T. F. Gallagher, *Phys. Rev. A* **35**, 2345 (1987).
- ³¹C. R. Mahon, G. R. Janik, and T. F. Gallagher, *Phys. Rev. A* **41**, 3746 (1990).
- ³²C. Bordsas, P. F. Brevet, M. Brojer, J. Chevalere, P. Labastie, and J. P. Perrott, *Phys. Rev. Lett.* **60**, 917 (1988).
- ³³J. M. Smith and W. A. Chupka, *J. Chem. Phys.* (to be published).
- ³⁴M. Bixon and J. Jortner (unpublished).
- ³⁵C. Alt, W. G. Scherzer, H. L. Selzle, and E. W. Schlag, *Chem. Phys. Lett.* (to be published).
- ³⁶R. N. Zare (private communication).
- ³⁷*Rydberg States of Atoms and Molecules*, edited by R. F. Stebbings and F. B. Dunning (Cambridge University, Cambridge, 1983).
- ³⁸H. A. Bethe and E. E. Salpeter, *Quantum Mechanics of One- and Two-Electron Atoms* (Springer, Berlin, 1957).
- ³⁹M. L. Zimmerman, M. G. Littman, M. M. Kash, and D. Kleppner, *Phys. Rev. A* **20**, 2251 (1979).
- ⁴⁰K. B. MacAdam, R. Rolfes, and D. A. Crosby, *Phys. Rev. A* **24**, 1286 (1981).
- ⁴¹K. B. MacAdam, R. G. Rolfes, X. Sun, J. Singh, W. L. Fuqua III, and D. B. Smith, *Phys. Rev. A* **36**, 4254 (1987).
- ⁴²X. Sun and K. B. MacAdam, *Phys. Rev. A* **47**, 3913 (1993).
- ⁴³I. L. Beigman and M. I. Syrkin, *Sov. Phys. JETP* **62**, 226 (1985).
- ⁴⁴I. Fischer, D. M. Villeneuve, M. J. J. Vrakking, and A. Stolow, *J. Chem. Phys.* **102**, 5566 (1995).

- ⁴⁵I. Fischer, M. J. J. Vrakking, D. M. Villeneuve, and A. Stolow (to be published).
- ⁴⁶M. C. R. Cockett (private communication).
- ⁴⁷D. M. Villeneuve, I. Fischer, and A. Stolow, *Opt. Commun.* **114**, 141 (1995).
- ⁴⁸For a review, see A. H. Zewail, *Femtochemistry-Ultrafast Dynamics of the Chemical Bond* (World Scientific, Singapore, 1994), Vols. I and II.
- ⁴⁹T. Baumert, R. Thalweiser, V. Weiss, and G. Gerber, in *Femtosecond Chemistry*, edited by J. Manz and L. Wöste (VCH, Weinheim, 1995).
- ⁵⁰M. Gruebele and A. H. Zewail, *J. Chem. Phys.* **98**, 883 (1993).
- ⁵¹J. W. Cooley, *Math Comput.* **XV**, 363 (1961).
- ⁵²G. Herzberg, *Spectra of Diatomic Molecules* (Van Nostrand, Princeton, 1950).
- ⁵³A. J. Yencha, M. C. R. Cockett, J. G. Goode, R. J. Donovan, A. Hopkirk, and G. C. King, *Chem. Phys. Lett.* **229**, 347 (1994).
- ⁵⁴H. Metiu and V. Engel, *J. Chem. Phys.* **93**, 5693 (1990).